


Cite this: *RSC Adv.*, 2018, 8, 26998

# Conversion of dilute nitrous oxide (N<sub>2</sub>O) in N<sub>2</sub> and N<sub>2</sub>–O<sub>2</sub> mixtures by plasma and plasma-catalytic processes†

Xing Fan, <sup>\*,a</sup> Sijing Kang,<sup>a</sup> Jian Li<sup>a</sup> and Tianle Zhu<sup>b</sup>

A coaxial dielectric barrier discharge (DBD) reactor has been developed for plasma and plasma-catalytic conversion of dilute N<sub>2</sub>O in N<sub>2</sub> and N<sub>2</sub>–O<sub>2</sub> mixtures at both room and high temperature (300 °C). The effects of catalyst introduction, O<sub>2</sub> content and inlet N<sub>2</sub>O concentration on N<sub>2</sub>O conversion and the mechanism involved in the conversion of N<sub>2</sub>O have been investigated. The results show that N<sub>2</sub>O in N<sub>2</sub> could be effectively decomposed to N<sub>2</sub> and O<sub>2</sub> by plasma and plasma-catalytic processes at both room and high temperature, with much higher decomposition efficiency at 300 °C than at room temperature for the same discharge power. Under an N<sub>2</sub>–O<sub>2</sub> atmosphere, however, N<sub>2</sub>O could be removed only at high temperature, producing not only N<sub>2</sub> and O<sub>2</sub> but also NO and NO<sub>2</sub>. Production and conversion of N<sub>2</sub>O occur simultaneously during the plasma and plasma-catalytic processing of N<sub>2</sub>O in a N<sub>2</sub>–O<sub>2</sub> mixture, with production and conversion being the dominant processes at room and high temperature, respectively. N<sub>2</sub>O conversion increases with the increase of discharge power and decreases with the increase of O<sub>2</sub> content. Increasing the inlet N<sub>2</sub>O concentration from 100 to 400 ppm decreases the conversion of N<sub>2</sub>O under an N<sub>2</sub> atmosphere but increases that under an N<sub>2</sub>–O<sub>2</sub> atmosphere. Concentrating N<sub>2</sub>O in the N<sub>2</sub>–O<sub>2</sub> mixture could alleviate the negative influence of O<sub>2</sub> by increasing the involvement of plasma reactive species (e.g., N<sub>2</sub>(A<sup>3</sup>Σ<sub>u</sub><sup>+</sup>) and O(<sup>1</sup>D)) in N<sub>2</sub>O conversion. Packing the discharge zone with a RuO<sub>2</sub>/Al<sub>2</sub>O<sub>3</sub> catalyst significantly enhances the conversion of N<sub>2</sub>O and improves the selectivity of N<sub>2</sub>O decomposition under an N<sub>2</sub>–O<sub>2</sub> atmosphere, revealing the synergy of plasma and catalyst in promoting N<sub>2</sub>O conversion, especially its decomposition to N<sub>2</sub> and O<sub>2</sub>.

Received 1st July 2018  
Accepted 21st July 2018

DOI: 10.1039/c8ra05607b

rsc.li/rsc-advances

## 1. Introduction

Nitrous oxide (N<sub>2</sub>O) emitted from various human activities including agriculture (soil cultivation and the use of nitrogen-fertilizers), biomass burning, fossil fuel combustion, industrial processes (production of adipic and nitric acids), and wastewater treatment is the third most significant anthropogenic greenhouse gas and the largest stratospheric-ozone-depleting substance.<sup>1–3</sup> Limiting the formation of N<sub>2</sub>O is the best solution to reduce N<sub>2</sub>O emissions from the agricultural sector and uncontrolled biomass burning taking into account the diffuse character of these emissions, while employment of after-treatment technologies is important for control of N<sub>2</sub>O emissions from combustion and industrial sources.<sup>3</sup>

Technologies developed and adopted so far for abatement of N<sub>2</sub>O are mainly based on catalysis, including non-selective

catalytic reduction (NSCR), selective catalytic reduction (SCR), and direct catalytic decomposition.<sup>1,3–8</sup> Among these technologies, the direct catalytic decomposition of N<sub>2</sub>O to N<sub>2</sub> and O<sub>2</sub> has received great attention due to simplicity and high efficiency and significant research efforts have been focused on development of novel catalytic materials with satisfactory activity at relatively low temperatures.<sup>1,3,5–8</sup> As a promising alternative to develop new catalysts, combination of catalysts with non-thermal plasma has been widely investigated in recent years for treatment of a variety of air contaminants such as volatile organic compounds (VOCs) and nitrogen oxides (NO<sub>x</sub>).<sup>9–16</sup> The synergetic effects between plasma and catalysis include initiating chemical reactions at low temperature and improving products selectivity.<sup>9–16</sup> In fact, plasma and plasma-catalysis systems have also been investigated for decomposition of N<sub>2</sub>O, with nitrogen or argon as the background gas in most cases.<sup>17–22</sup> These oxygen-free systems proved to be effective in decomposing N<sub>2</sub>O even at room temperature.<sup>17–22</sup> In real exhaust gases, however, O<sub>2</sub> always coexists with N<sub>2</sub>O and N<sub>2</sub> and it is therefore of great significance to investigate the N<sub>2</sub>O conversion behavior under N<sub>2</sub>–O<sub>2</sub> atmosphere.<sup>3</sup>

In a recent study by Jo *et al.*,<sup>23</sup> O<sub>2</sub> in N<sub>2</sub>–O<sub>2</sub>–N<sub>2</sub>O mixture was verified to have obviously adverse effects on the plasma-catalytic

<sup>a</sup>Key Laboratory of Beijing on Regional Air Pollution Control, College of Environmental and Energy Engineering, Beijing University of Technology, Beijing 100124, China. E-mail: fanxing@bjut.edu.cn

<sup>b</sup>School of Space and Environment, Beihang University, Beijing 100191, China

† Electronic supplementary information (ESI) available. See DOI: 10.1039/c8ra05607b



decomposition of  $\text{N}_2\text{O}$ . Besides the negative influence of  $\text{O}_2$  on the catalytic decomposition of  $\text{N}_2\text{O}$ , the intrinsic formation of  $\text{N}_2\text{O}$  by discharge in  $\text{N}_2\text{--O}_2$  should have also contributed to the decreasing  $\text{N}_2\text{O}$  conversion with increasing  $\text{O}_2$  content, which however was not taken into account in that study.<sup>23</sup> From our perspective, a better understanding of both  $\text{N}_2\text{O}$  production and conversion processes in the presence of  $\text{O}_2$  is essential for optimizing the plasma-catalytic decomposition of  $\text{N}_2\text{O}$ . On the other hand, Jo *et al.*<sup>23</sup> inferred from the thermodynamic calculations that  $\text{N}_2\text{O}$  was mainly decomposed into  $\text{N}_2$  and  $\text{O}_2$  in the presence of  $\text{O}_2$ . However, Krawczyk *et al.*<sup>24,25</sup> found that  $\text{N}_2\text{O}$  in mixtures with  $\text{O}_2$  or air was both oxidized to NO and decomposed to  $\text{N}_2$  and  $\text{O}_2$  by gliding arc discharge, combined with or without a catalytic bed. Oxidation of  $\text{N}_2\text{O}$  into NO and reusing NO for production of nitric acid is a profitable method for reducing concentrated  $\text{N}_2\text{O}$  emissions, *e.g.*, in adipic acid plants.<sup>24</sup> For removal of dilute  $\text{N}_2\text{O}$  from sources such as nitric acid production and fluidized bed combustion, however, decomposition of  $\text{N}_2\text{O}$  into  $\text{N}_2$  and  $\text{O}_2$  would be more desired.<sup>3</sup>

The aim of this study is to investigate the conversion behavior and mechanism of dilute  $\text{N}_2\text{O}$  in plasma and plasma-catalytic processes, in both the presence and absence of  $\text{O}_2$  and at both room and high temperature (300 °C). For this purpose, a coaxial dielectric barrier discharge (DBD) reactor was constructed, to generate plasma and to combine plasma with catalysts.  $\text{RuO}_2/\text{Al}_2\text{O}_3$  was chosen as the catalyst besides  $\text{Al}_2\text{O}_3$  for plasma-catalytic conversion of  $\text{N}_2\text{O}$  due to its reported good performance for catalytic  $\text{N}_2\text{O}$  decomposition.<sup>26</sup> The effects of catalyst ( $\text{Al}_2\text{O}_3$  or  $\text{RuO}_2/\text{Al}_2\text{O}_3$ ) introduction,  $\text{O}_2$  content (0–20%, volumetric) and inlet  $\text{N}_2\text{O}$  concentration (100–400 ppm, volumetric) on the conversion of  $\text{N}_2\text{O}$  were systematically examined. In order to elucidate the mechanism of  $\text{N}_2\text{O}$  conversion, the production of  $\text{N}_2\text{O}$  by discharge in  $\text{N}_2\text{--O}_2$  mixture with and without catalyst was also investigated and products/byproducts generated in these processes were analyzed in detail.

## 2. Experimental

### 2.1 Experimental set-up

A schematic diagram of the experimental system is shown in Fig. 1. It consists of reaction gas supply, a DBD reactor with an

alternating current (AC) high voltage power supply (0–100 kV, 50–500 Hz, sinusoidal wave), and analytical instrumentation. The reaction gas which was fed into the reactor at a total flow rate of 1 L  $\text{min}^{-1}$  at ambient temperature and pressure (around 20 °C, 100 kPa) throughout this work was prepared by mixing pure  $\text{N}_2$ ,  $\text{O}_2$ , and  $\text{N}_2\text{O}$  in  $\text{N}_2$  (Beijing HaiRui Tongda Gas Technology Co., Ltd., China) whose flow rates were controlled by a set of mass flow controllers (MFC, D07-7, Beijing Sevenstar Electronics Co., Ltd., China).  $\text{O}_2$  content in the feed gas was adjusted to 0%, 5%, 10% or 20% while inlet concentration of  $\text{N}_2\text{O}$  ranged from 0 to 400 ppm.

A quartz glass tube reactor (length: 600 mm; inner diameter: 29 mm; thickness: 1.5 mm) was used with a concentric tungsten wire (diameter: 1.4 mm) acting as the discharge electrode and an aluminum foil (50 mm in length) wrapping around the glass tube as the ground electrode. For the plasma-catalytic process,  $\text{Al}_2\text{O}_3$  or  $\text{RuO}_2/\text{Al}_2\text{O}_3$  catalyst pellets (20 g, 3–5 mm in diameter) were packed in the space between the discharge electrode and the tube at near maximum packing density, with an apparent volume of *ca.* 27 mL. The plasma/plasma-catalytic reactor was installed in normal indoor environments or in a temperature-controlled tube furnace to obtain room temperature and high temperature (300 °C) reaction conditions, respectively.

### 2.2 Experimental methods

#### 2.2.1 Preparation and characterization of catalyst.

Commercial  $\gamma\text{-Al}_2\text{O}_3$  pellets (Brunauer–Emmett–Teller (BET) specific surface area 226  $\text{m}^2 \text{g}^{-1}$ , specific pore capacity 0.48 mL  $\text{g}^{-1}$ , Tianjin Fuchen Chemical Reagents Factory, China) were used as the catalyst as well as the support of  $\text{RuO}_2/\text{Al}_2\text{O}_3$  catalyst. For the preparation of  $\text{RuO}_2/\text{Al}_2\text{O}_3$ , a given amount of  $\gamma\text{-Al}_2\text{O}_3$  pellets were impregnated with an aqueous solution of  $\text{RuCl}_3$  (99% purity, J&K Scientific). After the impregnation, drying overnight at 110 °C and calcining at 550 °C for 6 h in air atmosphere were performed. The nominal loading amount of Ru over  $\text{Al}_2\text{O}_3$  was 2.4 wt% and the BET specific surface area of the prepared  $\text{RuO}_2/\text{Al}_2\text{O}_3$  catalyst was 194  $\text{m}^2 \text{g}^{-1}$ , measured by  $\text{N}_2$  adsorption at –196 °C on a surface area and pore size analyzer (Micromeritics Gemini V, USA).

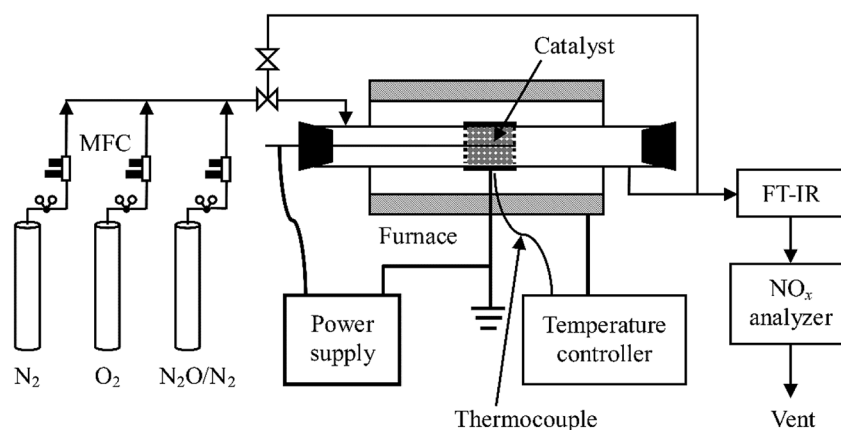


Fig. 1 Schematic diagram of the experimental set-up.



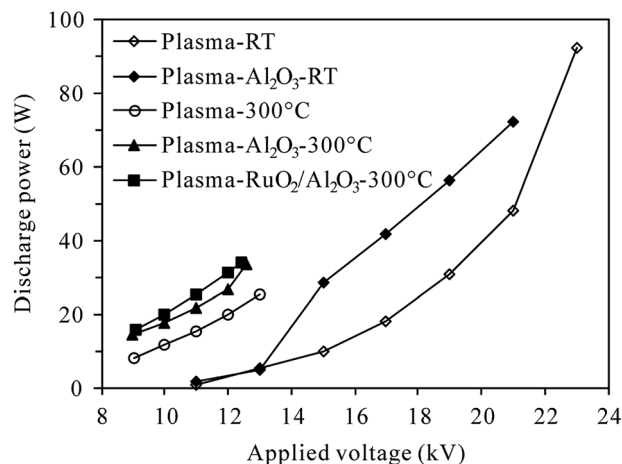


Fig. 2 Dependence of discharge power on the applied voltage at room temperature (RT) and 300 °C (inlet N<sub>2</sub>O: 0 ppm; O<sub>2</sub> content: 5%).

In addition, X-ray diffraction (XRD) patterns of Al<sub>2</sub>O<sub>3</sub> and RuO<sub>2</sub>/Al<sub>2</sub>O<sub>3</sub> catalysts before and after use in plasma-catalytic conversion of N<sub>2</sub>O were obtained using a Bruker D8 Discover diffractometer (Co K $\alpha$  radiation, 35 kV, 30 mA).

**2.2.2 Measurement of discharge characteristics.** The DBD reactor was energized at 200 Hz in the range of 9–23 kV (root-mean-square (RMS) value) in this study. The applied voltage and discharge current was measured using a 1000:1 high voltage probe (P6015A, Tektronix, USA) and a current monitor (UT61D, UNI-T, China), respectively. The discharge power delivered to the reactor was calculated by multiplying the time-dependent voltage and current. Fig. 2 presents typical discharge power values of plasma and plasma-catalytic reactors at room temperature and 300 °C as functions of applied voltage. It is worth pointing out that although higher discharge power could be delivered to the reactors under higher reaction temperature (300 °C) for a given applied voltage, the breakdown voltage and maximum applicable discharge power were much lower at 300 °C than those at room temperature.

**2.2.3 Analysis of gas components and calculation of N<sub>2</sub>O conversion.** The reactor outlet gas stream was analyzed using an on-line Fourier transform infrared (FT-IR) spectrometer (Nicolet iS10, Thermo-Scientific, USA) equipped with a heated gas cell (optical path length: 2.4 m; volume: 300 mL; temperature: 100 °C) and a deuterated triglycine sulfate (DTGS) KBr detector. Spectra were recorded automatically every 35 s (average of 16 scans from 4000 to 650 cm<sup>-1</sup> with a resolution of 4 cm<sup>-1</sup>) from the start to the end of each experiment, with the background spectra being recorded under dry N<sub>2</sub> before the experiment. For quantification of N<sub>2</sub>O, NO and NO<sub>2</sub>, the FT-IR spectrometer was calibrated using standard gases of these components, with measurement uncertainty of  $\pm 1$  ppm. Besides, NO and NO<sub>2</sub> concentrations were also measured by a NO<sub>x</sub> analyzer (42i-HL, Thermo-Scientific, USA, uncertainty  $\pm 1\%$ ). Considering the relative low infrared absorption of NO and potential interference by H<sub>2</sub>O, concentration of NO was mainly determined by the NO<sub>x</sub> analyzer in this work while that of NO<sub>2</sub> by the FT-IR spectrometer.

The conversion of N<sub>2</sub>O is calculated based on its inlet (C<sub>N<sub>2</sub>O,in</sub>, ppm) and outlet concentrations (C<sub>N<sub>2</sub>O,out</sub>, ppm), as shown in eqn (1).

$$\text{Conversion of N}_2\text{O} = \frac{C_{\text{N}_2\text{O,in}} - C_{\text{N}_2\text{O,out}}}{C_{\text{N}_2\text{O,in}}} \times 100\% \quad (1)$$

The selectivity of NO, NO<sub>2</sub> and NO<sub>x</sub> (NO + NO<sub>2</sub>) produced from N<sub>2</sub>O conversion is calculated based on the N-balance as follows:

$$\text{Selectivity of NO} = \frac{C_{\text{NO,with N}_2\text{O}} - C_{\text{NO,w/o N}_2\text{O}}}{2 \times (C_{\text{N}_2\text{O,in}} - C_{\text{N}_2\text{O,out}})} \times 100\% \quad (2)$$

$$\text{Selectivity of NO}_2 = \frac{C_{\text{NO}_2,\text{with N}_2\text{O}} - C_{\text{NO}_2,\text{w/o N}_2\text{O}}}{2 \times (C_{\text{N}_2\text{O,in}} - C_{\text{N}_2\text{O,out}})} \times 100\% \quad (3)$$

$$\text{Selectivity of NO}_x = \text{selectivity of NO} + \text{selectivity of NO}_2 \quad (4)$$

where C<sub>NO,with N<sub>2</sub>O</sub>, C<sub>NO,w/o N<sub>2</sub>O</sub> and C<sub>NO<sub>2</sub>,with N<sub>2</sub>O</sub>, C<sub>NO<sub>2</sub>,w/o N<sub>2</sub>O</sub> indicate the outlet concentrations of NO and NO<sub>2</sub> (ppm) detected with and without N<sub>2</sub>O in the inlet gas, respectively; 2 is the number ratio of nitrogen atoms of N<sub>2</sub>O and NO/NO<sub>2</sub>.

## 3. Results and discussion

### 3.1 Conversion of N<sub>2</sub>O at room temperature

**3.1.1 Conversion of N<sub>2</sub>O under N<sub>2</sub> atmosphere.** Fig. 3 shows the conversion of 100 ppm-N<sub>2</sub>O in N<sub>2</sub> as functions of discharge power in plasma and plasma-Al<sub>2</sub>O<sub>3</sub> reactors at room temperature. It can be seen that without O<sub>2</sub> in the reaction gas, N<sub>2</sub>O can be effectively decomposed by both plasma and plasma-Al<sub>2</sub>O<sub>3</sub> processes. The N<sub>2</sub>O conversion increased with the increase of discharge power, which can be easily ascribed to the

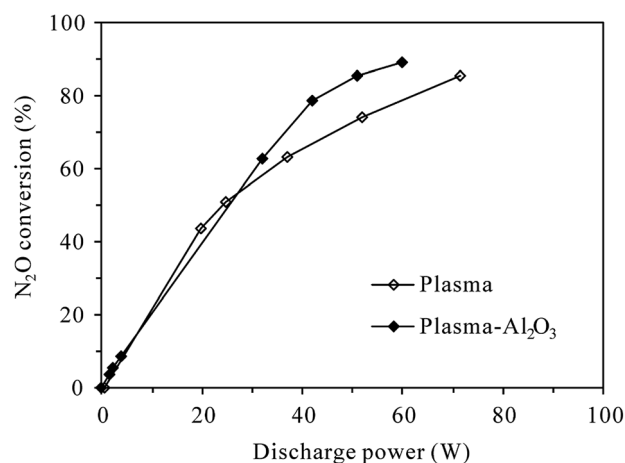
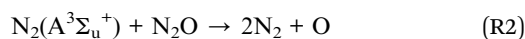
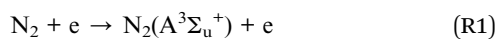


Fig. 3 Dependence of N<sub>2</sub>O conversion on the discharge power in plasma and plasma-Al<sub>2</sub>O<sub>3</sub> reactors at room temperature (inlet N<sub>2</sub>O: 100 ppm; O<sub>2</sub> content: 0%).



increment of active species for  $\text{N}_2\text{O}$  decomposition at higher discharge power. In an intensive study of  $\text{N}_2\text{O}$  conversion by pulsed corona discharge in  $\text{N}_2$ , Zhao *et al.*<sup>18</sup> confirmed that among the active species, the first excited state of molecular nitrogen, *i.e.*,  $\text{N}_2(\text{A}^3\Sigma_u^+)$  produced by electron impact excitation of nitrogen molecules (reaction (R1)<sup>27</sup>), appeared to be mainly involved in the decomposition of  $\text{N}_2\text{O}$  through reaction (R2). Reaction (R2) was also concluded to be responsible for the conversion of  $\text{N}_2\text{O}$  in  $\text{N}_2$  DBD plasma by Trinh *et al.*<sup>20</sup> With the increase of discharge power, more  $\text{N}_2(\text{A}^3\Sigma_u^+)$  would be produced for  $\text{N}_2\text{O}$  decomposition due to the increase of energetic electrons. As shown in Fig. 3, the highest  $\text{N}_2\text{O}$  conversion was 85.7% and 89.4% observed at the highest discharge power of 71.6 W and 59.8 W tested for plasma and plasma- $\text{Al}_2\text{O}_3$  process, respectively. Packing with  $\text{Al}_2\text{O}_3$  catalyst slightly facilitated the decomposition of  $\text{N}_2\text{O}$  in  $\text{N}_2$ , probably by enhancing the electric fields around the contact points of dielectric  $\text{Al}_2\text{O}_3$  pellets.<sup>19</sup>



**3.1.2 Conversion and production of  $\text{N}_2\text{O}$  under  $\text{N}_2$ - $\text{O}_2$  atmosphere.** Once  $\text{O}_2$  (5%, 10% or 20%) was added into the reaction gas,  $\text{N}_2\text{O}$  could not be decomposed anymore at room temperature, no matter in the presence or absence of  $\text{Al}_2\text{O}_3$  catalyst. In fact,  $\text{N}_2\text{O}$  concentration increased due to additional production of  $\text{N}_2\text{O}$ , which was widely accepted to proceed mainly by the reaction of  $\text{N}_2(\text{A}^3\Sigma_u^+)$  with oxygen, as shown in (R3).<sup>27–29</sup> Obviously,  $\text{N}_2(\text{A}^3\Sigma_u^+)$  plays an important role in both production and decomposition of  $\text{N}_2\text{O}$  *via* (R3) and (R2), respectively.

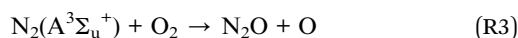


Fig. 4 compares the increased concentration of  $\text{N}_2\text{O}$  ( $C_{\text{N}_2\text{O},\text{out}} - C_{\text{N}_2\text{O},\text{in}}$ ) under different  $\text{O}_2$  contents with and without 100 ppm- $\text{N}_2\text{O}$  in the  $\text{N}_2$ - $\text{O}_2$  mixture. As can be seen from Fig. 4(a), no matter with or without  $\text{N}_2\text{O}$  in the inlet gas, the increased concentration of  $\text{N}_2\text{O}$  in the plasma reactor first increased and then decreased with the increase of discharge power, attaining a maximum at *ca.* 35 W. The reason for this may be that the increase of discharge power promotes not only the formation of  $\text{N}_2\text{O}$  *via* (R3), but also  $\text{N}_2\text{O}$  loss by (R2) and/or (R4)–(R6).<sup>27,29–31</sup> Higher discharge power means that more energy could be used to excite/dissociate  $\text{N}_2$  and  $\text{O}_2$  molecules, producing more reactive species such as  $\text{N}_2(\text{A}^3\Sigma_u^+)$  and  $\text{O}(\text{D})$ . At relatively low discharge power, the concentration of  $\text{N}_2\text{O}$  increased with increasing discharge power due to the enhanced production of  $\text{N}_2(\text{A}^3\Sigma_u^+)$  species for  $\text{N}_2\text{O}$  formation (R3). With the increase of  $\text{N}_2\text{O}$  concentration and increasing production of reactive species ( $\text{N}_2(\text{A}^3\Sigma_u^+)$  and  $\text{O}(\text{D})$ ), the probability of  $\text{N}_2\text{O}$  loss reactions ((R2), (R5) and (R6)) raised, explaining the observed decrease of  $\text{N}_2\text{O}$  concentration at higher discharge power. In the whole discharge power range tested, however, the production of  $\text{N}_2\text{O}$  surpassed the loss since the increased concentration of  $\text{N}_2\text{O}$  was always positive.

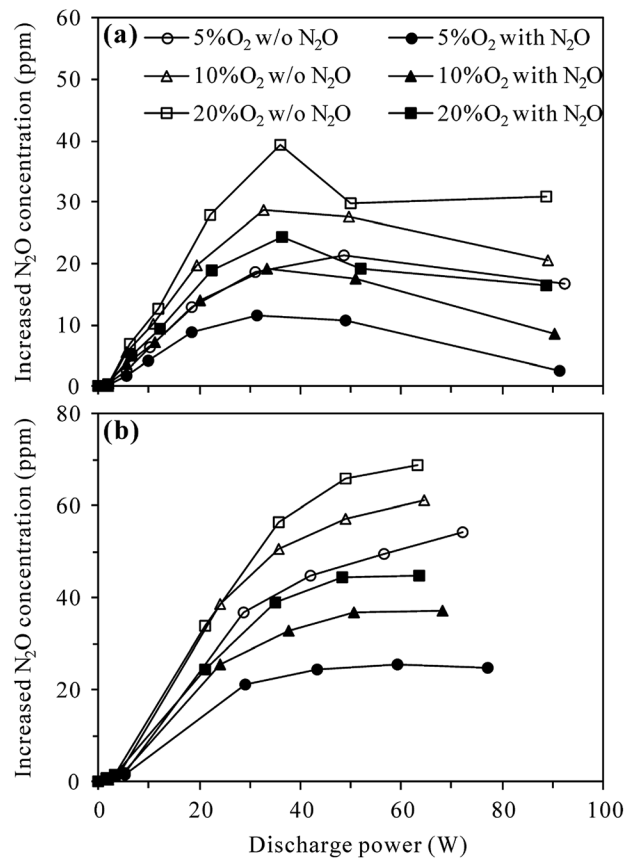


Fig. 4 Effects of  $\text{N}_2\text{O}$  presence in  $\text{N}_2$ - $\text{O}_2$  mixture on the production of  $\text{N}_2\text{O}$  by discharge in (a) plasma and (b) plasma- $\text{Al}_2\text{O}_3$  reactors at room temperature (inlet  $\text{N}_2\text{O}$ : 0 or 100 ppm;  $\text{O}_2$  content: 5%, 10% or 20%).

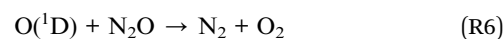
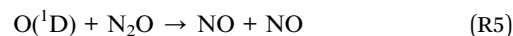
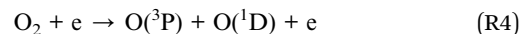
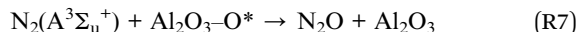


Fig. 4(a) also shows that in both the presence and absence of  $\text{N}_2\text{O}$  in the inlet gas, more  $\text{N}_2\text{O}$  was produced in the plasma reactor under higher  $\text{O}_2$  contents for a given discharge power, indicating the important role of  $\text{O}_2$  in  $\text{N}_2\text{O}$  production.<sup>27,29</sup> Compared with the case without  $\text{N}_2\text{O}$  in the inlet gas, introduction of 100 ppm- $\text{N}_2\text{O}$  significantly reduced the production of  $\text{N}_2\text{O}$  under all  $\text{O}_2$  contents. In the presence of initial  $\text{N}_2\text{O}$ , more  $\text{N}_2(\text{A}^3\Sigma_u^+)$  species would be consumed in  $\text{N}_2\text{O}$  decomposition (reaction (R2)), reducing the amount of  $\text{N}_2(\text{A}^3\Sigma_u^+)$  species for  $\text{N}_2\text{O}$  production (reaction (R3)) as a result.

Compared to plasma alone, more  $\text{N}_2\text{O}$  was produced in the plasma- $\text{Al}_2\text{O}_3$  reactor (Fig. 4(b)) under otherwise similar conditions, indicating the promotion effects of  $\text{Al}_2\text{O}_3$  catalyst on  $\text{N}_2\text{O}$  formation by discharge. In a study focusing on  $\text{N}_2\text{O}$  formation by DBD in  $\text{N}_2$ - $\text{O}_2$  mixtures, Tang *et al.* also reported similar increase of  $\text{N}_2\text{O}$  production by packing  $\text{Al}_2\text{O}_3$  in the discharge zone and surface oxygen species ( $\text{Al}_2\text{O}_3\text{-O}^*$ ) brought by  $\text{Al}_2\text{O}_3$



into the plasma chemical process (reaction (R7)) was considered as the main reason.<sup>29</sup>



where \* represents an active site on the catalyst and O\* represents atomic oxygen bound to the site.<sup>29</sup>

In the presence of  $\text{Al}_2\text{O}_3$  catalyst (Fig. 4(b)), the increased concentration of  $\text{N}_2\text{O}$  first increased and then tended to reach equilibrium values with the increase of discharge power, demonstrating that  $\text{N}_2\text{O}$  production was counterbalanced by  $\text{N}_2\text{O}$  loss at high discharge power, especially when  $\text{N}_2\text{O}$  was introduced into the inlet gas. As in the plasma case, introduction of 100 ppm- $\text{N}_2\text{O}$  into the  $\text{N}_2\text{-O}_2$  mixture also resulted in less production of  $\text{N}_2\text{O}$  in the plasma- $\text{Al}_2\text{O}_3$  reactor (Fig. 4(b)).

In addition, it is worth mentioning that although the presence of 100 ppm- $\text{N}_2\text{O}$  in the  $\text{N}_2\text{-O}_2$  mixture significantly affected the production of  $\text{N}_2\text{O}$  by discharge, it did not induce significant changes to the formation behavior of NO and  $\text{NO}_2$  in both plasma (Fig. S1†) and plasma- $\text{Al}_2\text{O}_3$  reactors (Fig. S2†) at room temperature.

### 3.2 Conversion of $\text{N}_2\text{O}$ at high temperature

In order to decompose  $\text{N}_2\text{O}$  in the  $\text{O}_2$ -containing atmosphere, the reaction temperature was raised to 300 °C in this section and  $\text{RuO}_2/\text{Al}_2\text{O}_3$  was also investigated besides  $\text{Al}_2\text{O}_3$  for plasma-catalytic decomposition of  $\text{N}_2\text{O}$ .

**3.2.1 Effects of catalyst introduction.** Fig. 5 presents the conversion of  $\text{N}_2\text{O}$  in plasma and plasma-catalytic reactors as functions of discharge power at 300 °C. The concentrations of  $\text{N}_2\text{O}$  and  $\text{O}_2$  in the inlet gas were 400 ppm and 5%, respectively. In the absence of plasma (at discharge power of 0 W), a small conversion of  $\text{N}_2\text{O}$  (1.8%) was observed in the plasma- $\text{RuO}_2/\text{Al}_2\text{O}_3$  reactor while no  $\text{N}_2\text{O}$  was converted in the plasma or plasma- $\text{Al}_2\text{O}_3$  reactors. This indicated that  $\text{N}_2\text{O}$  was stable in the gas phase and over the  $\text{Al}_2\text{O}_3$  catalyst at as high as 300 °C, but

$\text{RuO}_2/\text{Al}_2\text{O}_3$  catalyst did show low activity for  $\text{N}_2\text{O}$  decomposition. The conversion of  $\text{N}_2\text{O}$  increased with the increase of discharge power no matter the catalyst was introduced or not, demonstrating that  $\text{N}_2\text{O}$  in  $\text{N}_2\text{-O}_2$  mixture could indeed be removed by plasma and plasma-catalytic processes at high temperature. When no catalyst was packed in the discharge zone, however, the  $\text{N}_2\text{O}$  conversion was very low, reaching only 3.8% at the highest discharge power tested (21.8 W). Introducing catalyst, especially  $\text{RuO}_2/\text{Al}_2\text{O}_3$  into the discharge zone greatly improved the conversion of  $\text{N}_2\text{O}$ . Considering that  $\text{Al}_2\text{O}_3$  and  $\text{RuO}_2/\text{Al}_2\text{O}_3$  catalysts alone showed no or very low activity for  $\text{N}_2\text{O}$  decomposition at 300 °C, the enhanced conversion of  $\text{N}_2\text{O}$  in the plasma-catalytic process could only be attributed to the synergy of plasma and catalyst in  $\text{N}_2\text{O}$  conversion.<sup>23,24</sup> The highest conversion of  $\text{N}_2\text{O}$ , however, was only 31.2% observed in the plasma- $\text{RuO}_2/\text{Al}_2\text{O}_3$  reactor. As stated in Section 2.2.2, the maximum applicable discharge power was limited at 300 °C due to easy breakdown of the reactor wall material (quartz glass). Further increase of the discharge power and  $\text{N}_2\text{O}$  conversion may be achieved by using reactors with higher resistance to breakdown, such as alumina ceramic tube reactor.<sup>23</sup>

On the other hand, Fig. 6 shows the production of  $\text{N}_2\text{O}$  in the plasma and plasma-catalytic processes at 300 °C without  $\text{N}_2\text{O}$  in the inlet gas (inlet gas composition: 5%  $\text{O}_2 + \text{N}_2$ ). It can be seen that for both plasma and plasma-catalytic processes,  $\text{N}_2\text{O}$  concentration increased almost linearly with discharge power in the range tested. Packing catalyst in the discharge zone greatly enhanced the production of  $\text{N}_2\text{O}$ , but no significant difference was observed in  $\text{N}_2\text{O}$  production between the plasma- $\text{Al}_2\text{O}_3$  and plasma- $\text{RuO}_2/\text{Al}_2\text{O}_3$  systems. Compared to the room-temperature case (Fig. 4), much less  $\text{N}_2\text{O}$  was produced at 300 °C for the same  $\text{O}_2$  content (5%) and discharge power. Considering the low conversion of  $\text{N}_2\text{O}$  obtained, especially in the plasma and plasma- $\text{Al}_2\text{O}_3$  processes (Fig. 5), the observed less production of  $\text{N}_2\text{O}$  (Fig. 6) should be mainly due to the low effectiveness of  $\text{N}_2\text{O}$  formation reactions (e.g., (R3)) at high temperature. In other words, high reaction temperature is

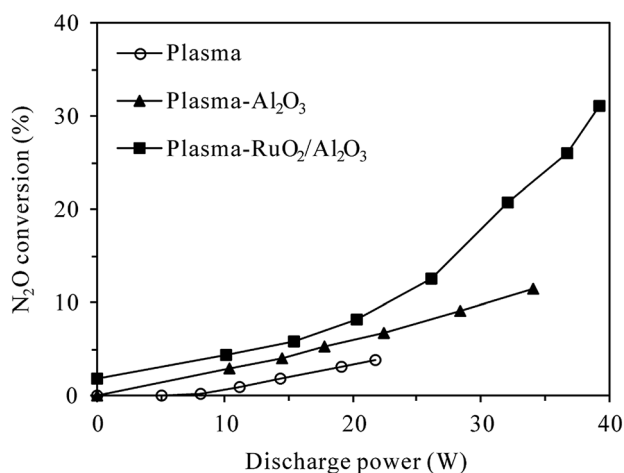


Fig. 5 Dependence of  $\text{N}_2\text{O}$  conversion on the discharge power in plasma and plasma-catalytic reactors at 300 °C (inlet  $\text{N}_2\text{O}$ : 400 ppm;  $\text{O}_2$  content: 5%).

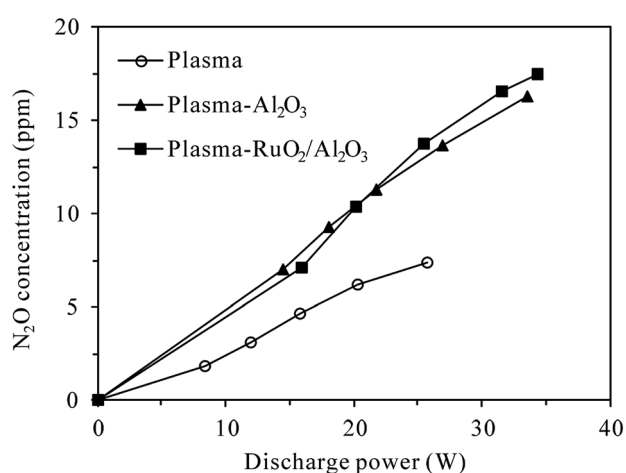


Fig. 6 Dependence of  $\text{N}_2\text{O}$  production on the discharge power in plasma and plasma-catalytic reactors at 300 °C (inlet  $\text{N}_2\text{O}$ : 0 ppm;  $\text{O}_2$  content: 5%).



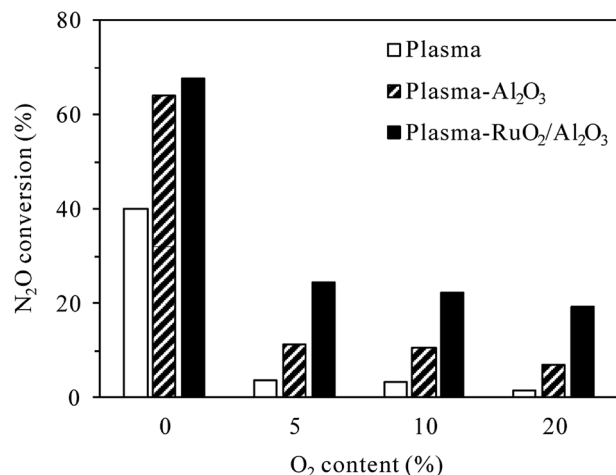
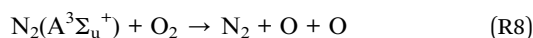


Fig. 7 Effects of O<sub>2</sub> content on N<sub>2</sub>O conversion in plasma and plasma-catalytic reactors at 300 °C (inlet N<sub>2</sub>O: 400 ppm; discharge power: 22 W for the plasma process and 34 W for the plasma-catalytic process).

favorable not only for conversion of N<sub>2</sub>O but also for reduction of N<sub>2</sub>O formation by discharge in N<sub>2</sub>-O<sub>2</sub> mixture. At high temperature (300 °C), introducing catalyst, especially RuO<sub>2</sub>/Al<sub>2</sub>O<sub>3</sub> into the discharge zone significantly enhances the conversion of N<sub>2</sub>O, overbalancing its promoting effects on N<sub>2</sub>O production, which finally results in effective removal of N<sub>2</sub>O from the N<sub>2</sub>-O<sub>2</sub> mixture (Fig. 5).

**3.2.2 Effects of O<sub>2</sub> content.** O<sub>2</sub> content can largely influence the plasma/plasma-catalytic conversion of N<sub>2</sub>O due to the intrinsic formation of N<sub>2</sub>O in N<sub>2</sub>-O<sub>2</sub> plasma. Fig. 7 shows the effects of O<sub>2</sub> content on N<sub>2</sub>O conversion (inlet N<sub>2</sub>O 400 ppm) in plasma and plasma-catalytic processes at 300 °C. In both the presence and absence of catalyst, the conversion of N<sub>2</sub>O drastically decreased when the O<sub>2</sub> content was changed from 0 to 5%, revealing that O<sub>2</sub> inhibited the plasma and plasma-catalytic decomposition of N<sub>2</sub>O significantly. Jo *et al.*<sup>23</sup> attributed the negative influence of O<sub>2</sub> on catalytic and plasma-catalytic decomposition of N<sub>2</sub>O to the competitive adsorption of O<sub>2</sub> onto the active sites over RuO<sub>2</sub>/Al<sub>2</sub>O<sub>3</sub> catalyst. Besides this, O<sub>2</sub> could significantly decrease the electron density and the formation rate of N<sub>2</sub>(A<sup>3</sup>Σ<sub>u</sub><sup>+</sup>) species in plasma due to its electronegative characteristics.<sup>32–35</sup> In addition to directly react with N<sub>2</sub>(A<sup>3</sup>Σ<sub>u</sub><sup>+</sup>) species to produce additional N<sub>2</sub>O (reaction (R3)), O<sub>2</sub> could also reduce the amount of N<sub>2</sub>(A<sup>3</sup>Σ<sub>u</sub><sup>+</sup>) species by dissociative quenching (reaction (R8)) due to its low dissociation energy (5.2 eV per molecule).<sup>32,36</sup> The decrease of N<sub>2</sub>(A<sup>3</sup>Σ<sub>u</sub><sup>+</sup>) species for N<sub>2</sub>O decomposition, additional production of N<sub>2</sub>O as well as the competitive adsorption of O<sub>2</sub> over the catalyst sites should all contribute to the dramatic decrease of N<sub>2</sub>O conversion in the presence of O<sub>2</sub>.



As also shown in Fig. 7, for the same discharge power of 34 W, N<sub>2</sub>O conversion in the plasma-Al<sub>2</sub>O<sub>3</sub> process decreased from 64.3% for 0% O<sub>2</sub> content to 11.4% for 5% O<sub>2</sub> content,

while that in the plasma-RuO<sub>2</sub>/Al<sub>2</sub>O<sub>3</sub> process decreased from 67.9% to 24.4%. The superiority of RuO<sub>2</sub>/Al<sub>2</sub>O<sub>3</sub> over Al<sub>2</sub>O<sub>3</sub> was more pronounced in the O<sub>2</sub>-containing cases. Further increase of the O<sub>2</sub> content from 5% to 10% and 20% caused further decrease of the N<sub>2</sub>O conversion, but the extent of decrease was less prominent.

**3.2.3 Effects of inlet N<sub>2</sub>O concentration.** The inlet concentration of N<sub>2</sub>O can also be an important factor influencing the plasma and plasma-catalytic decomposition processes. The effects of inlet N<sub>2</sub>O concentration on N<sub>2</sub>O conversion at 300 °C with 0% and 5% O<sub>2</sub> in the reaction gas are presented in Fig. 8. For the plasma process (Fig. 8(a)), at a given discharge power of 22 W, the conversion of N<sub>2</sub>O without O<sub>2</sub> significantly decreased from 71.6% to 40.0% while that with 5% O<sub>2</sub> slightly increased from 1.2% to 3.8% when the inlet N<sub>2</sub>O concentration was increased from 100 to 400 ppm. It is obvious that higher inlet concentration leads to lower conversion of N<sub>2</sub>O in N<sub>2</sub> plasma due to the competitive consumption of reactive species for N<sub>2</sub>O decomposition (N<sub>2</sub>(A<sup>3</sup>Σ<sub>u</sub><sup>+</sup>)) by increasing N<sub>2</sub>O molecules. In the presence of 5% O<sub>2</sub>, however, the conversion of N<sub>2</sub>O was enhanced by injecting more N<sub>2</sub>O into the reaction gas. The reason for this may be that more N<sub>2</sub>(A<sup>3</sup>Σ<sub>u</sub><sup>+</sup>) species would be consumed in the decomposition of higher-concentration N<sub>2</sub>O

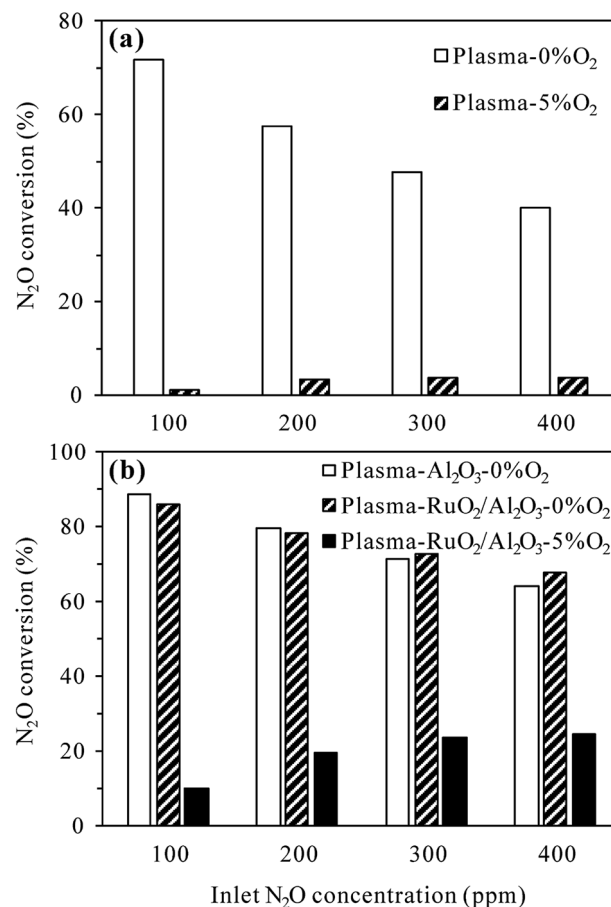


Fig. 8 Effects of inlet N<sub>2</sub>O concentration on N<sub>2</sub>O conversion in (a) plasma and (b) plasma-catalytic reactors at 300 °C (O<sub>2</sub> content: 0% or 5%; discharge power: 22 W for the plasma process and 34 W for the plasma-catalytic process).



(reaction (R2)), reducing the amount of  $N_2(A^3\Sigma_u^+)$  species for  $N_2O$  formation (reaction (R3)).

For the plasma-catalytic process (Fig. 8(b)), at a given discharge power of 34 W, the conversion of  $N_2O$  without  $O_2$  also decreased with increasing inlet  $N_2O$  concentration, but the decrease was less significant compared to that in the plasma process, proving the higher capacity of plasma-catalytic process in decomposing  $N_2O$ . Besides, it was noticed that the difference in the  $N_2O$  conversion between the plasma- $Al_2O_3$  and plasma- $RuO_2/Al_2O_3$  processes was insignificant in the absence of  $O_2$ , indicating the minor role of  $RuO_2$  in promoting  $N_2O$  decomposition under  $N_2$  atmosphere although  $RuO_2$  greatly improved the  $N_2O$  conversion under  $N_2-O_2$  atmosphere (Fig. 5 and 7).

As in the plasma process (Fig. 8(a)), the conversion of  $N_2O$  in the plasma- $RuO_2/Al_2O_3$  process also increased with the increase of inlet  $N_2O$  concentration in the presence of 5%  $O_2$ , especially from 100 to 200 and 300 ppm (Fig. 8(b)). Further increasing the inlet  $N_2O$  concentration, e.g., to 400 ppm, showed limited effects in enhancing the  $N_2O$  conversion, probably due to the limited amount of reactive species ( $N_2(A^3\Sigma_u^+)$  and  $O(^1D)$ ) produced under a given discharge power for  $N_2O$  conversion. From the point of fully utilizing the generated reactive species and reducing the negative influence of  $O_2$  on  $N_2O$  conversion, dilute  $N_2O$  in  $N_2-O_2$  mixture should be concentrated, e.g., by adsorption-desorption process before being converted by the plasma-catalytic process.<sup>20</sup>

In addition, it is noteworthy that for the same inlet  $N_2O$  concentration of 100 ppm and background gas of  $N_2$ ,  $N_2O$  conversion in the plasma process increased from 47.1% at room temperature (Fig. 3) to 71.6% at 300 °C (Fig. 8(a)) for the same discharge power of 22 W. Similarly,  $N_2O$  conversion in the plasma- $Al_2O_3$  process increased from 66.2% at room temperature (Fig. 3) to 88.7% at 300 °C (Fig. 8(b)) for the same discharge power of 34 W. These results suggest that  $N_2O$  in  $N_2$  could be decomposed more efficiently by plasma and plasma-catalytic processes at higher reaction temperature.

### 3.3 Mechanism of $N_2O$ conversion

**3.3.1  $N_2O$  conversion pathways.** On-line FT-IR (Fig. S3†) and  $NO_x$  measurement results show that under  $N_2$  atmosphere, no other nitrogen oxide species were produced during the plasma and plasma-catalytic decomposition of  $N_2O$  regardless of the reaction temperature. O radicals generated in (R2) should have recombined and/or reacted with  $N_2O$  ((R6)) to give out  $O_2$  as the final product instead of being consumed for  $NO/NO_2$  production. In other words,  $N_2O$  was degraded to  $N_2$  and  $O_2$  by discharge in  $N_2$  in both the presence and absence of catalyst and at both room and high temperature. Trinh *et al.*<sup>20</sup> proposed similar mechanism for direct decomposition of  $N_2O$  in  $N_2$  DBD plasma.

On the other hand, as stated in Section 3.2,  $N_2O$  in  $N_2-O_2$  mixture could be removed by plasma and plasma-catalytic processes only at high temperature. Fig. S4† shows typical FT-IR spectra of the effluents of plasma and plasma-catalytic reactors with and without 400 ppm- $N_2O$  in the inlet gas ( $O_2$  content 5%) and before and after discharge at 300 °C. Clearly,

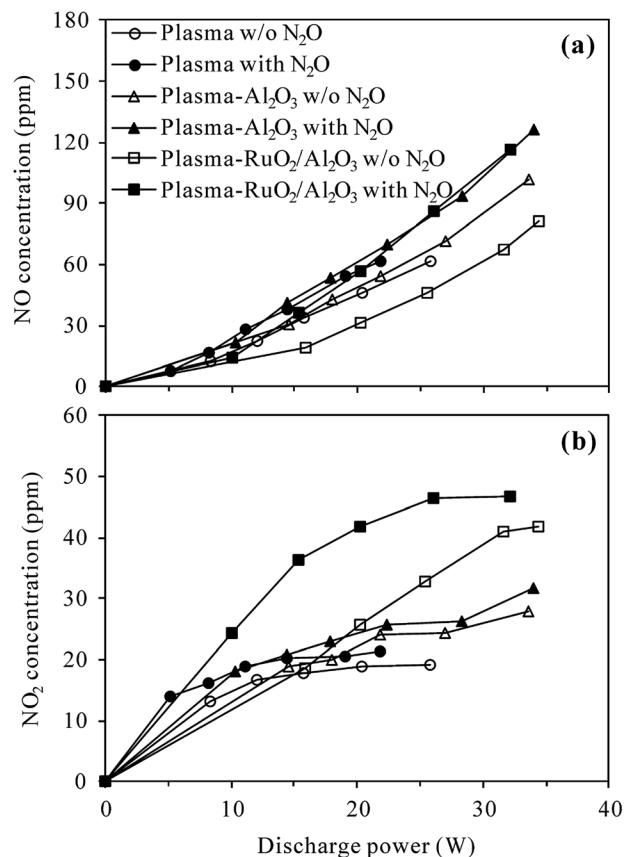


Fig. 9 Concentrations of (a) NO and (b)  $NO_2$  formed with and without 400 ppm  $N_2O$  in the inlet gas of plasma and plasma-catalytic reactors at 300 °C ( $O_2$  content: 5%).

discharge in  $N_2-O_2$  mixture at 300 °C produced  $N_2O$ , NO and  $NO_2$  as byproducts no matter the catalyst was present or not. When  $N_2O$  was introduced into the  $N_2-O_2$  mixture, NO and  $NO_2$  were also detected besides the residual  $N_2O$ . In order to clarify whether  $N_2O$  was converted to NO and  $NO_2$  under  $N_2-O_2$  atmosphere, the outlet concentrations of NO and  $NO_2$  detected with and without 400 ppm- $N_2O$  in the inlet gas were compared in Fig. 9.

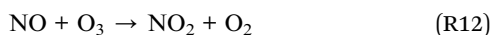
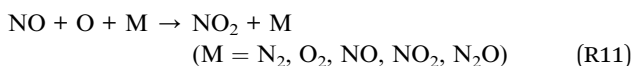
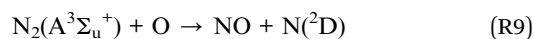
Overall, NO and  $NO_2$  concentrations increased with the increase of discharge power and the presence of 400 ppm- $N_2O$  in the  $N_2-O_2$  mixture did not obviously change the variation trends of NO or  $NO_2$  concentrations. For a given discharge power, however, higher concentrations of NO and  $NO_2$  were always detected when  $N_2O$  was introduced, especially in the plasma- $RuO_2/Al_2O_3$  process. This result revealed that  $N_2O$  was partially transformed into NO and  $NO_2$  during the  $O_2$ -containing conversion processes, being in agreement with the observations of Krawczyk *et al.*<sup>24,25</sup> Table 1 lists the selectivity of NO,  $NO_2$  and  $NO_x$  ( $NO + NO_2$ ) at typical discharge power in the plasma and plasma-catalytic processes. As seen, the selectivity of  $NO_x$  ranged from 28.7% of the plasma- $Al_2O_3$  process at 34.0 W to 79.5% of the plasma process at 14.4 W. Other removed  $N_2O$  should have been degraded to benign  $N_2$  and  $O_2$  since no N-containing byproducts other than NO and  $NO_2$  were observed.



**Table 1** Selectivity of NO, NO<sub>2</sub> and NO<sub>x</sub> (NO + NO<sub>2</sub>) at typical discharge power in plasma and plasma-catalytic processes (inlet N<sub>2</sub>O: 400 ppm; O<sub>2</sub> content: 5%; reaction temperature: 300 °C)

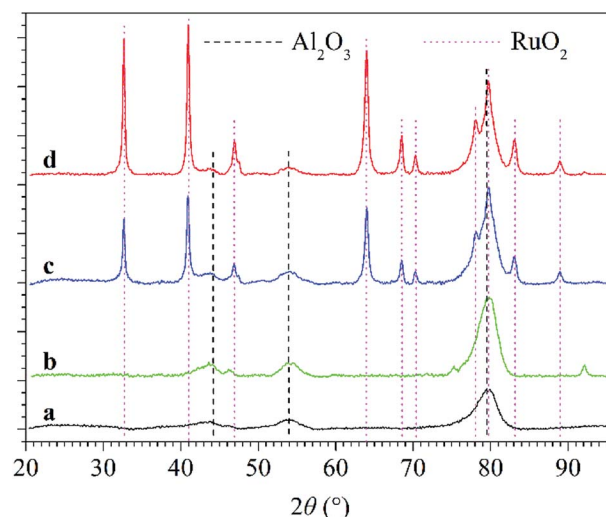
Process	Discharge power (W)	Selectivity of NO (%)	Selectivity of NO <sub>2</sub> (%)	Selectivity of NO <sub>x</sub> (%)
Plasma	14.4	59.2	20.3	79.5
	21.8	37.1	7.6	44.7
Plasma-Al <sub>2</sub> O <sub>3</sub>	14.4	34.0	6.5	40.5
	34.0	24.7	4.0	28.7
Plasma-RuO <sub>2</sub> /Al <sub>2</sub> O <sub>3</sub>	15.4	36.9	38.7	75.6
	32.1	28.4	3.4	31.8

Table 1 also shows that compared to the plasma process, the selectivity of NO<sub>x</sub> was relatively low in the plasma-catalytic process, indicating that catalyst packed in the discharge zone promoted N<sub>2</sub>O decomposition to N<sub>2</sub> and O<sub>2</sub> to a larger extent than oxidation to NO and NO<sub>2</sub>. For all processes, the selectivity of NO and NO<sub>2</sub> decreased with the increase of discharge power, probably due to the substantial increase of NO and NO<sub>2</sub> formation from plasma-induced reactions between N<sub>2</sub> and O<sub>2</sub> which competitively consumed oxidative species, as shown in reactions (R9)–(R12).<sup>27,29,32,37</sup> Besides, the selectivity of NO was much higher than that of NO<sub>2</sub> except at low discharge power of the plasma-RuO<sub>2</sub>/Al<sub>2</sub>O<sub>3</sub> process. This can be easily ascribed to the step-wise oxidation of N<sub>2</sub>O (first (R5) and then (R11) and (R12)) under oxidative plasma atmosphere.<sup>27,32,37</sup>



Compared to Al<sub>2</sub>O<sub>3</sub> catalyst, RuO<sub>2</sub>/Al<sub>2</sub>O<sub>3</sub> catalyst significantly enhanced the selectivity of NO<sub>2</sub> at low discharge power. At higher discharge power, however, the difference in the selectivity of NO and NO<sub>2</sub> between the two plasma-catalytic processes became insignificant. At the relatively high discharge power tested, more than 40% and *ca.* 30% of the removed nitrogen in N<sub>2</sub>O was transformed into NO<sub>x</sub> in the plasma and plasma-catalytic process, respectively.

**3.3.2 Synergy mechanism of plasma and catalyst for N<sub>2</sub>O conversion under N<sub>2</sub>–O<sub>2</sub> atmosphere.** From the above-mentioned analysis, it can be concluded that introducing catalyst, especially RuO<sub>2</sub>/Al<sub>2</sub>O<sub>3</sub> into the discharge zone significantly enhanced the conversion of N<sub>2</sub>O and promoted N<sub>2</sub>O decomposition to N<sub>2</sub> and O<sub>2</sub> under N<sub>2</sub>–O<sub>2</sub> atmosphere. Fig. 10 shows the XRD patterns of Al<sub>2</sub>O<sub>3</sub> and RuO<sub>2</sub>/Al<sub>2</sub>O<sub>3</sub> catalysts before and after use in plasma-catalytic conversion of N<sub>2</sub>O at 300 °C. From the XRD analysis, cubic Al<sub>2</sub>O<sub>3</sub> was observed for all catalyst samples and tetragonal RuO<sub>2</sub> was formed over the RuO<sub>2</sub>/Al<sub>2</sub>O<sub>3</sub> catalyst. For both Al<sub>2</sub>O<sub>3</sub> and RuO<sub>2</sub>/Al<sub>2</sub>O<sub>3</sub> catalysts, the XRD patterns were almost unchanged after use, indicating



**Fig. 10** XRD patterns of Al<sub>2</sub>O<sub>3</sub> and RuO<sub>2</sub>/Al<sub>2</sub>O<sub>3</sub> catalysts: (line a) fresh Al<sub>2</sub>O<sub>3</sub> catalyst; (line b) Al<sub>2</sub>O<sub>3</sub> catalyst after use in plasma-catalytic conversion of N<sub>2</sub>O at 300 °C; (line c) fresh RuO<sub>2</sub>/Al<sub>2</sub>O<sub>3</sub> catalyst; (line d) RuO<sub>2</sub>/Al<sub>2</sub>O<sub>3</sub> catalyst after use in plasma-catalytic conversion of N<sub>2</sub>O at 300 °C.

that neither plasma nor the N<sub>2</sub>O conversion reactions changed the phase composition of the catalysts.

According to literatures, the decomposition of N<sub>2</sub>O over metal oxide catalysts can be expressed as a Langmuir–Hinshelwood mechanism:



where \* stands for an active site of the catalyst.<sup>3,23</sup> In this mechanism, the adsorbed surface oxygen (O\*) migrates from one active site to another to form O<sub>2</sub> by recombination, which is known to be the rate-determining step.<sup>3,23</sup> Applying DBD plasma in the RuO<sub>2</sub>/Al<sub>2</sub>O<sub>3</sub> catalyst bed could not only initiate gas-phase conversion of N<sub>2</sub>O ((R2), (R5) and (R6)), but also accelerate the catalytic conversion of N<sub>2</sub>O by speeding up the consumption of adsorbed surface oxygen (O\*), *e.g.*, via reaction (R15) to regenerate the active sites.<sup>23</sup> In fact, the scavenging of O\* by O radicals (reaction (R15)) also explained the decreased selectivity of NO<sub>x</sub>



(increased selectivity of N<sub>2</sub> and O<sub>2</sub>) in the presence of catalyst (Table 1), revealing the synergy of plasma and catalyst in promoting N<sub>2</sub>O decomposition.



## 4. Conclusions

In the present work, conversion of dilute N<sub>2</sub>O in N<sub>2</sub> and N<sub>2</sub>-O<sub>2</sub> mixtures by plasma and plasma-catalytic processes was investigated at both room and high temperature (300 °C). It is found that N<sub>2</sub>O in N<sub>2</sub> can be effectively decomposed to N<sub>2</sub> and O<sub>2</sub> by plasma and plasma-catalytic processes at both room and high temperature, with much higher decomposition efficiency at 300 °C than at room temperature for the same discharge power. However, N<sub>2</sub>O in N<sub>2</sub>-O<sub>2</sub> mixture can be removed only at high temperature, producing not only N<sub>2</sub> and O<sub>2</sub> but also NO and NO<sub>2</sub>. Production and conversion of N<sub>2</sub>O occur simultaneously during the plasma and plasma-catalytic processing of N<sub>2</sub>O in N<sub>2</sub>-O<sub>2</sub> mixture, with production and conversion being the dominant process at room and high temperature, respectively.

N<sub>2</sub>O conversion increases with the increase of discharge power and decreases with the increase of O<sub>2</sub> content. The negative influence of O<sub>2</sub> on N<sub>2</sub>O conversion could be suppressed to some extent by concentrating N<sub>2</sub>O in N<sub>2</sub>-O<sub>2</sub> mixture which increases the involvement of plasma reactive species (e.g., N<sub>2</sub>(A<sup>3</sup>Σ<sub>u</sub><sup>+</sup>) and O(<sup>1</sup>D)) in N<sub>2</sub>O conversion. Introducing catalyst, especially RuO<sub>2</sub>/Al<sub>2</sub>O<sub>3</sub> into the discharge zone significantly enhances the conversion of N<sub>2</sub>O and improves the selectivity of N<sub>2</sub>O decomposition under N<sub>2</sub>-O<sub>2</sub> atmosphere, revealing the synergy of plasma and catalyst in promoting N<sub>2</sub>O conversion, especially its decomposition to N<sub>2</sub> and O<sub>2</sub>. The combined plasma-catalytic processing may be an efficient way for reducing N<sub>2</sub>O emissions from combustion and industrial sources.

## Conflicts of interest

There are no conflicts to declare.

## Acknowledgements

This work was supported by the National Natural Science Foundation of China (grant numbers 21707004, 51638001) and the Natural Science Foundation of Beijing Municipality (grant number 8152011).

## References

- 1 J. Pérez-Ramírez, F. Kapteijn, K. Schöffel and J. A. Moulijn, *Appl. Catal., B*, 2003, **44**, 117–151.
- 2 K. R. Sistani, M. Jn-Baptiste, N. Lovanh and K. L. Cook, *J. Environ. Qual.*, 2011, **40**, 1797–1805.
- 3 M. Konsolakis, *ACS Catal.*, 2015, **5**, 6397–6421.
- 4 A. Ates, A. Reitzmann, C. Hardacre and H. Yalcin, *Appl. Catal., A*, 2011, **407**, 67–75.

- 5 F. Zhang, X. Wang, X. Zhang, M. Turxun, H. Yu and J. Zhao, *Chem. Eng. J.*, 2014, **256**, 365–371.
- 6 M. Konsolakis, F. Aligizou, G. Goula and I. V. Yentekakis, *Chem. Eng. J.*, 2013, **230**, 286–295.
- 7 S. S. Kim, S. J. Lee and S. C. Hong, *Chem. Eng. J.*, 2011, **169**, 173–179.
- 8 Z. Liu, C. He, B. Chen and H. Liu, *Catal. Today*, 2017, **297**, 78–83.
- 9 H. L. Chen, H. M. Lee, S. H. Chen, M. B. Chang, S. J. Yu and S. N. Li, *Environ. Sci. Technol.*, 2009, **43**, 2216–2227.
- 10 J. V. Durme, J. Dewulf, C. Leys and H. V. Langenhove, *Appl. Catal., B*, 2008, **78**, 324–333.
- 11 X. Fan, T. L. Zhu, Y. F. Sun and X. Yan, *J. Hazard. Mater.*, 2011, **196**, 380–385.
- 12 Y. J. Wan, X. Fan and T. L. Zhu, *Chem. Eng. J.*, 2011, **171**, 314–319.
- 13 X. Fan, T. L. Zhu, Y. J. Wan and X. Yan, *J. Hazard. Mater.*, 2010, **180**, 616–621.
- 14 X. Fan, T. L. Zhu, M. Y. Wang and X. M. Li, *Chemosphere*, 2009, **75**, 1301–1306.
- 15 Q. Yu, Y. Gao, X. Tang, H. Yi, R. Zhang, S. Zhao, F. Gao and Y. Zhou, *Catal. Commun.*, 2018, **110**, 18–22.
- 16 A. Mizuno, *Catal. Today*, 2013, **211**, 2–8.
- 17 X. Hu, J. Nicholas, J. Zhang, T. M. Linjewile, P. D. Filippis and P. K. Agarwal, *Fuel*, 2002, **81**, 1259–1268.
- 18 G. B. Zhao, X. D. Hu, M. D. Argyle and M. Radosz, *Ind. Eng. Chem. Res.*, 2004, **43**, 5077–5088.
- 19 S. Mahammadunnisa, E. L. Reddy, P. R. M. K. Reddy and C. Subrahmanyam, *Plasma Processes Polym.*, 2013, **10**, 444–450.
- 20 Q. Trinh, S. H. Kim and Y. S. Mok, *Chem. Eng. J.*, 2016, **302**, 12–22.
- 21 D. H. Lee and T. Kim, N<sub>2</sub>O decomposition by catalyst-assisted cold plasma, *20th Int. Symp. Plasma Chem.*, Philadelphia, USA, 2012.
- 22 H. Hu, H. Huang, J. Xu, Q. Yang and G. Tao, *Plasma Sci. Technol.*, 2015, **17**, 1043–1047.
- 23 J. Jo, Q. H. Trinh, S. H. Kim and Y. S. Mok, *Catal. Today*, 2018, **310**, 42–48.
- 24 K. Krawczyk and M. Młotek, *Appl. Catal., B*, 2001, **30**, 233–245.
- 25 K. Schmidt-Szałowski, K. Krawczyk and M. Młotek, *J. Adv. Oxid. Technol.*, 2007, **10**, 330–336.
- 26 G. Pekridis, C. Athanasiou, M. Konsolakis, I. V. Yentekakis and G. E. Marnellos, *Top. Catal.*, 2009, **52**, 1880–1887.
- 27 I. A. Kossyi, A. Y. Kostinsky, A. A. Matveyev and V. P. Silakov, *Plasma Sources Sci. Technol.*, 1992, **1**, 207–220.
- 28 M. P. Iannuzzi, J. B. Jeffries and F. Kaufman, *Chem. Phys. Lett.*, 1982, **87**, 570–574.
- 29 X. Tang, J. Wang, H. Yi, S. Zhao, F. Gao, Y. Huang, R. Zhang and Z. Yang, *Energy Fuels*, 2017, **31**, 13901–13908.
- 30 J. T. Herron and D. S. Green, *Plasma Chem. Plasma Process.*, 2001, **21**, 459–481.
- 31 K. Krawczyk, *IEEE Trans. Plasma Sci.*, 2009, **37**, 884–889.
- 32 G. B. Zhao, S. Garikipati, X. D. Hu, M. D. Argyle and M. Radosz, *AIChE J.*, 2005, **51**, 1800–1812.



- 33 G. Sathiamoorthy, S. Kalyana, W. C. Finney, R. J. Clark and B. R. Locke, *Ind. Eng. Chem. Res.*, 1999, **38**, 1844–1855.
- 34 S. Kanazawa, J. S. Chang, G. F. Round, G. Sheng, T. Ohkubo, Y. Nomoto and T. Adachi, *J. Electrostat.*, 1997, **40–41**, 651–656.
- 35 Y. S. Mok, J. H. Kim, I. S. Nam and S. W. Ham, *Ind. Eng. Chem. Res.*, 2000, **39**, 3938–3944.
- 36 M. S. Bak, W. Kim and M. A. Cappelli, *Appl. Phys. Lett.*, 2011, **98**, 011502.
- 37 Y. Zhang, X. Tang, H. Yi, Q. Yu, J. Wang, F. Gao, Y. Gao, D. Li and Y. Cao, *RSC Adv.*, 2016, **6**, 63946–63953.

